CHEMISTRY OF MATERIALS

pubs.acs.org/cm

Article

Ammoniate Intermediates Enable Tunable Biphasic Molten Salt/Organic Synthesis of Colloidal GaN Nanocrystals

James Cassidy, Ruiming Lin, Alexandra Krupinski, Maia Czaikowski, Wooje Cho, John S. Anderson, and Dmitri V. Talapin*

Cite This: https://doi.org/10.1021/acs.chemmater.5c03186

Read Online

ACCESS | Metrics & More | Article Recommendations | Supporting Information

ABSTRACT: We report a systematic investigation into the biphasic synthesis of gallium nitride (GaN) nanocrystals using molten gallium halide salts and organic amines, with a particular focus on the role of ammoniate intermediates as viable precursors for GaN quantum dot synthesis. By systematically varying the identity of organic amine and the ammonia-to-gallium ratio in GaN biphasic reactions, we elucidate key parameters governing GaN formation, phase selectivity, and size control. Ammonia was shown to be convenient for nitride formation, with GaI_3 readily forming gallium ammoniate intermediates upon exposure. These intermediates, particularly in their lower-ammoniate forms (e.g., $GaI_3 \cdot 1NH_3$), enabled GaN nucleation upon heating, while higher-order ammoniates (e.g., $GaI_3 \cdot 7NH_3$) were unable to nucleate new crystalline GaN but participated in the growth of GaN nanocrystals. By adjusting the ratio of nucleation-initiating to growth-directing ammoniate precursors, nanocrystal diameters could be tuned from 2 to 12 nm. Additionally, halides present during the synthesis provide control over nanocrystal phase (i.e., zinc blende vs wurtzite). These results provide new insights into the complex reactivity landscape of GaN colloidal synthesis and establish ammoniate intermediates as key precursors for producing tunable III−N nanocrystals.

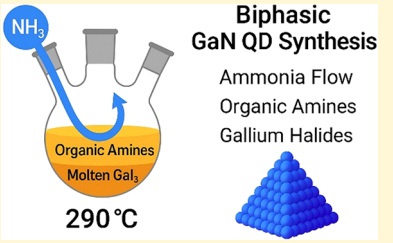

INTRODUCTION

Group III-nitride semiconductors (GaN, InGaN, etc.) are among the world's most technologically important materials for solid-state lighting, power electronics, and display technologies, due to their tunable bandgap in visible wavelengths, high stability, and low toxicity.[1−3] Currently, III-nitride semiconductors are manufactured by chemical vapor deposition (CVD) for epitaxially grown thin films or via the ammonothermal method using supercritical ammonia to grow bulk crystals.[4] Thin-film crystal growth of GaN via CVD requires temperatures of 800 °C−1200 °C, while ammonothermal bulk crystal growth uses 400 °C−650 °C temperatures in combination with 100 MPa−500 MPa of pressure, which makes both these technologies for GaN synthesis restrictive in scale and expense.[5,6] The preparation of III-nitrides by colloidal solution synthesis would bring dramatic cost reductions through scaling of homogeneous solution synthesis, combined with the benefits of nonepitaxial device integration, additive manufacturing capabilities, and optical tunability via size, shape, and composition control.

To date, the number of publications on colloidal GaN nanocrystals has been limited since no viable routes presently exist for the scalable synthesis of high-quality quantum dots suitable for application in optoelectronic devices. An early report showed that using cyclotrigallazane as a single source processor could produce nanocrystalline GaN via a pyrolysis route.[7] However, while the pyrolysis reaction begins at 180 °C, it is not complete until temperatures >500 °C,[7] an unrealistic temperature for an organic solvent-based approach. Another single source precursor, gallium imide powder with the formula $[Ga(NH)_{3/2}]_n$, is an alternative reagent first synthesized in 1996 by the reaction of tris(dimethylamino)gallium dimer with ammonia. Gallium imide was found to form nanocrystalline GaN under ammonia flow at 500 °C via pyrolysis.[8] Mićić et al. reported the first colloidal synthesis of GaN by refluxing gallium imide in trioctylamine (TOA) under ammonia atmosphere.[9] This approach was later modified by eliminating the need for ammonia and refluxing tris(dimethylamino)-gallium dimer in trioctylamine with the addition of hexadecylamine (HDA).[10] The use of a primary amine was found to be critical in synthesizing GaN from tris(dimethylamino)gallium dimer, although the end results are comparable to those originally obtained by Mićić et al. The downside of these colloidal pyrolysis methods is that they require high temperatures >330 °C applied for several days, which causes decomposition of organic solvents and contamination of the formed GaN with carbonaceous impurities, as well as little to no control over nanocrystal size and sample uniformity.

Received: November 25, 2025
Revised: March 27, 2026
Accepted: April 1, 2026

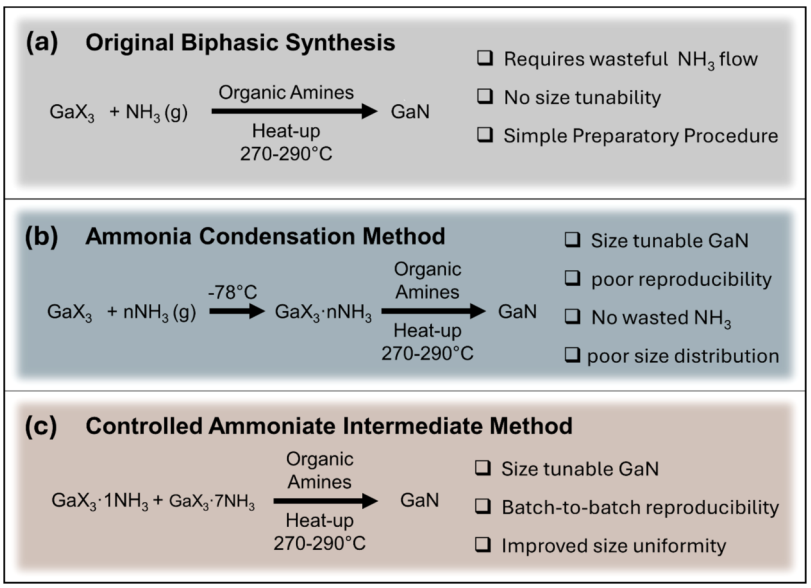

Figure 1. Overview of biphasic synthetic routes for GaN nanocrystals. (a) Originally reported method,[20] which relies on a continuous flow of ammonia gas, resulting in significant ammonia waste. Under ambient ammonia pressures, only a single nanocrystal size is accessible. (b) Modified approach in which a controlled amount of ammonia is first condensed onto gallium iodide, followed by the addition of organic amines (e.g., a 4:1 mixture of trioctylamine and hexadecylamine). In this method, the size of the as-synthesized GaN nanocrystals can be tuned by varying the amount of condensed ammonia: larger quantities yield larger nanocrystals, while smaller quantities produce smaller nanocrystals. This approach also eliminates the need for large excesses of ammonia gas. (c) The most refined biphasic method. By combining low-order gallium ammoniates (e.g., $GaI_3 \cdot 1NH_3$) with high-order gallium ammoniates (e.g., $GaI_3 \cdot 7NH_3$), the size of the resulting GaN nanocrystals can be readily controlled. Low-order ammoniates favor nucleation, whereas high-order ammoniates promote nanocrystal growth. This also results in nanocrystals with more well-defined morphologies and improved size distribution.

For a more controlled colloidal approach, Sardar and Rao reported the solvothermal reaction of gallium-Cupferron complex or gallium chloride with hexamethyldisilazane (HMDS) using toluene pressurized in a steel autoclave.[11] Similarly, Choi et al. employed gallium stearate with lithium bis(trimethylsilyl)amide in 1-octadecene as a solvent in order to synthesize both GaN and zinc doped GaN nanocrystals at 280 °C.[12] Both of these methods use oxygen containing species (Cupferron and stearic acid, respectively) which introduces the possibility of contaminating GaN with oxygen. The presence of impurities from synthetic conditions has a significant impact on the photophysical properties of GaN. The band gap of bulk wurtzite GaN is 3.4 eV at 300 K, and high quality CVD grown GaN films show band-edge photo- and electroluminescence centered at 365 nm.[13] In contrast, many reports on colloidally synthesized GaN nanocrystals have shown broad emission spectra with photoluminescence (PL) maxima at longer wavelengths.[11,14−17] Similar broad emission features, known as "yellow luminescence" in GaN, have been observed and extensively studied in defective CVD-grown GaN.[13,18] While the exact origin of yellow-band emission in GaN crystals is still debated, the emerging body of work suggests that carbon impurities on the N-sublattice, Ga vacancies, oxygen incorporation, as well as other defects, all contribute to the emergence of a broad visible emission of GaN.[18,19]

To advance the colloidal synthesis of GaN, our group has developed a novel method for producing crystalline gallium nitride (GaN) and aluminum nitride (AlN) nanocrystals using a biphasic mixture of high-boiling organic solvents and molten inorganic salts as the reaction medium, as outlined in Figure 1a.[20] By leveraging this biphasic system under an ammonia atmosphere at moderate temperatures (below 300 °C), we successfully synthesized GaN and AlN nanocrystals. These nanocrystals were functionalized with organic ligands post-synthetically, ensuring their colloidal stability in organic solvents. This approach improved crystallinity and phase purity of nanocrystals, thus paving the way for the scalable production of III-nitride nanomaterials, with promising applications in electronic and optoelectronic devices.

Herein, we further investigate gallium halide reactions in organic amines to reveal the chemical origin of challenges in the colloidal synthesis of Ga pnictide nanocrystals in organic solvents in contrast to the well-characterized growth of indium pnictide nanocrystals.[21−23] Next, we explore the biphasic synthesis of GaN using different organic amines, revealing that the addition of primary or secondary alkylamines provides improved crystallinity and enables a more tunable synthesis of GaN compared to that with tertiary amines. Furthermore, we draw insights from ammonothermal GaN synthesis in supercritical ammonia, introducing fluoride as a powerful surfactant and exploring ammonia coordination number to gallium ions to tune the shape and phase of GaN nanocrystals, as described in Figure 1b,c. This study expands our understanding and control of the biphasic GaN synthesis, demonstrating size-tunable growth of GaN quantum dots (QDs) with structural control of zinc blende versus wurtzite phase content.

RESULTS AND DISCUSSION

General Considerations for Colloidal Synthesis of Gallium Pnictides

A key question in colloidal synthesis of III−V nanocrystals is why are indium-based pnictides (InN, InP, InAs, InSb) readily synthesized via colloidal methods, while gallium-based

https://doi.org/10.1021/acs.chemmater.5c03186
Chem. Mater. XXXX, XXX, XXX−XXX

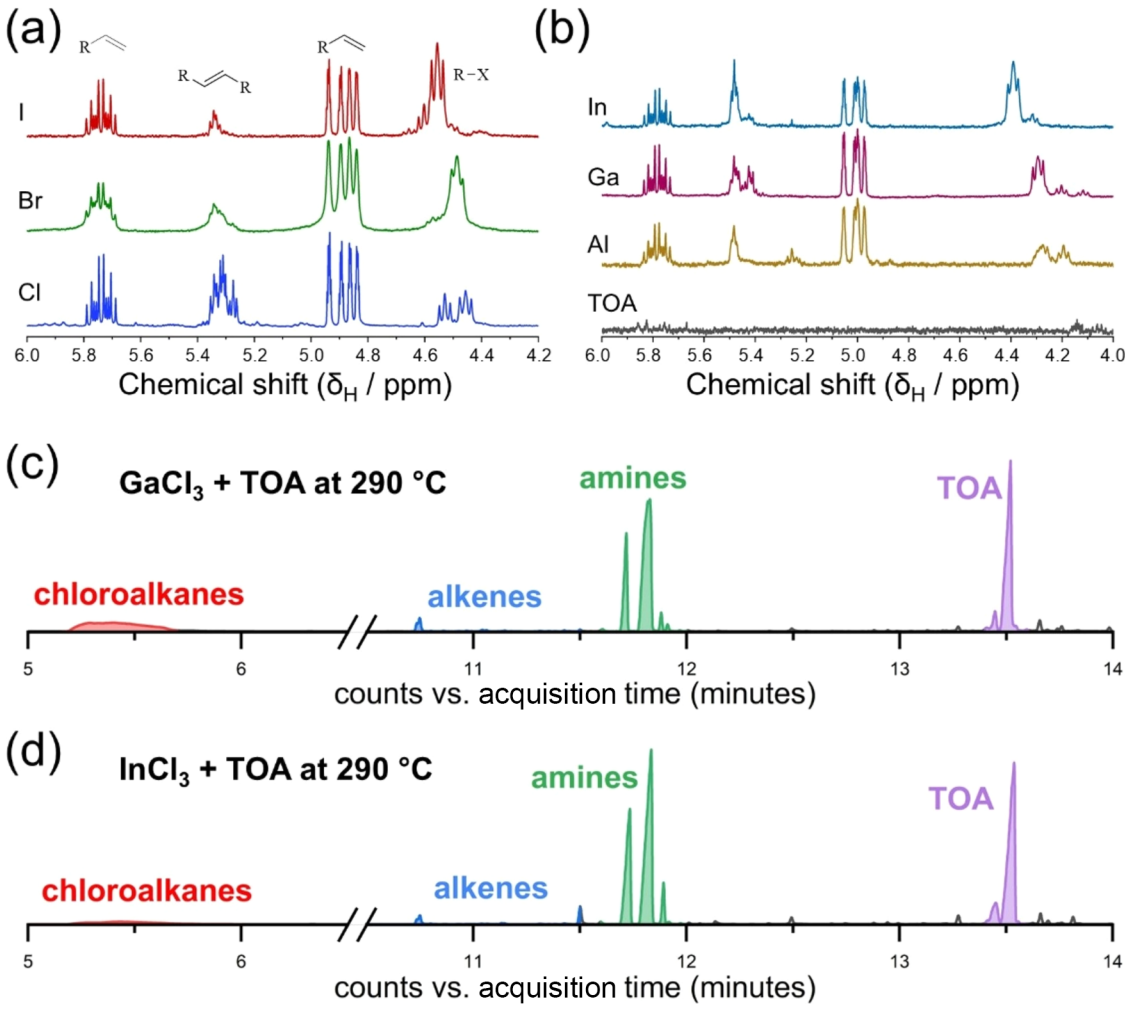

Figure 2. Overview of the products of TOA degradation in the presence of metal halides. Experiments were performed by heating 1 mmol of metal halide salt in 1 mL of TOA at 290 °C for 1 h. (a) ^{1}H NMR comparison of $InCl_3$, $GaCl_3$, and $AlCl_3$ relative to neat TOA in deuterated benzene. (b) Effect of metal halide identity on the observed degradation products in ^{1}H NMR in deuterated chloroform. (c) GC-MS data from a mixture of gallium chloride (1 mol equiv) in trioctylamine (3 mol equiv) heated at 290 °C for 1 h. (d) GC-MS data from a mixture of indium chloride (1 mol equiv) in trioctylamine (3 mol equiv) heated at 290 °C for 1 h.

pnictides continue to present significant synthetic challenges? We believe the answer is multifold. First, gallium(III) species are more oxophilic compared to indium(III) and can readily form oxides by reacting with carboxylates and other oxygen-containing precursors and surface ligands commonly used in colloidal synthesis. Specifically, previous work utilizing thermogravimetric analysis (TGA) has shown that gallium stearate begins to decompose below 200 °C, which is significantly lower than the decomposition temperature (>300 °C) for indium stearate.[24] As a consequence, metal carboxylates are widely used precursors in colloidal synthesis of indium pnictides,[25,26] but gallium carboxylates cannot be used as a precursor in high-temperature synthesis due to the formation of gallium oxide. Indeed, an attempt to synthesize GaN from gallium chloride, stearic acid, and ammonia produced spinel gallium oxynitride as the main product instead of GaN.[12] Therefore, successful synthesis of phase-pure GaN nanocrystals would require elimination of all oxygen-containing reagents, which can be achieved by using anhydrous gallium halides (e.g., $GaCl_3$) and long-chain alkylamines, such as trioctylamine (TOA) as a high-boiling solvent and *n*-hexadecylamine (HDA) as a surface ligand.

We investigated the behavior of gallium halide salts ($GaCl_3$, $GaBr_3$, GaI_3) when heated in TOA at 300 °C (Figures 1a and S1a). All three solutions exhibited visible reflux at this temperature, demonstrating the degradation of TOA, which has a boiling point of 365 °C. ^{1}H NMR spectra of the TOA-GaX_3 solutions (X = Cl, Br, I for gallium metal salts) revealed the appearance of new chemical shifts between 4 and 6 ppm that were otherwise absent in the original TOA, indicating the formation of new species. To further understand these peaks, we performed additional reactions using a series of metal chloride salts ($AlCl_3$, $GaCl_3$, $InCl_3$) (Figures 1b and S1b). Across these experiments, most of the observed chemical shifts remained consistent regardless of the halide or metal used. However, the region between 4.2 and 4.6 ppm exhibited strong halide-dependent variation, suggesting the presence of halogen-containing compounds. This region is commonly associated with alkenes and halocarbons. Based on coupling patterns, the peaks at 5.7 and 4.9 ppm were consistent with terminal alkenes. This assignment was additionally supported by ^{13}C NMR and comparison with a 1-octene reference, which both showed corresponding chemical shifts at 139 and 114 ppm (Figure S2). Further evidence was provided by gas

https://doi.org/10.1021/acs.chemmater.5c03186
Chem. Mater. XXXX, XXX, XXX−XXX

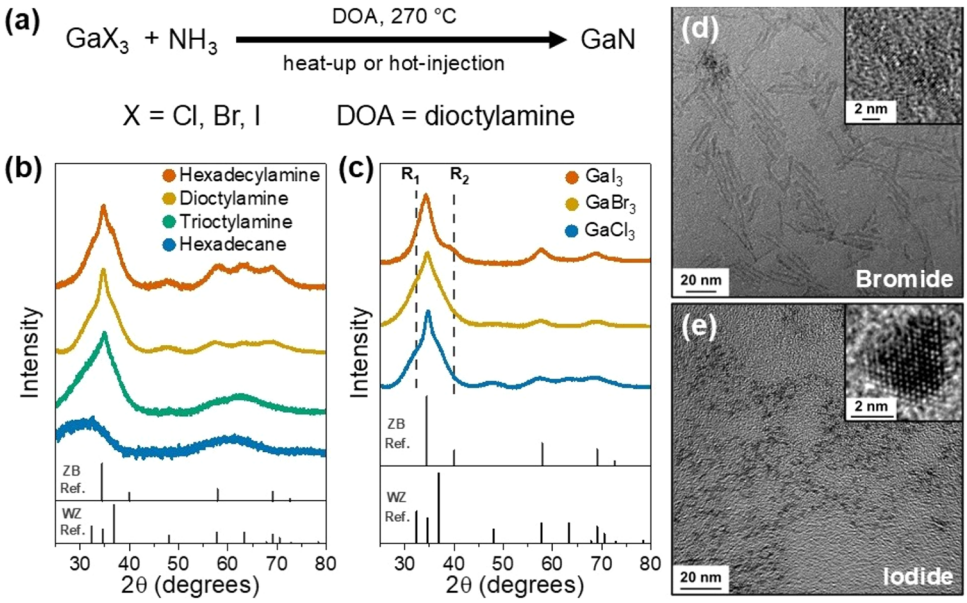

Figure 3. Overview of the biphasic synthesis of GaN nanocrystals. (a) The reaction schematic when using dioctylamine (DOA). (b) Powder X-ray diffraction (PXRD) patterns of GaN synthesized using $GaCl_3$ in the presence of primary, secondary, and tertiary amines. Results from the synthesis in the presence of hexadecane are also included, demonstrating the importance of organic amines. (c) Powder X-ray diffraction (PXRD) patterns of GaN synthesized using different gallium halide salts. Chloride and bromide salts lead to the synthesis of wurtzite (wz) nanorods as evidenced by the narrowing of the (0002) diffraction peak and clear presence of the wz (1011) peak highlighted by reference line 1 (R_1). Iodide salt produced zinc blende (zb) spheroidal nanocrystals as evidenced by the emergence of the zb (002) diffraction peak highlighted by reference line 2 (R_2) which is absent in the chloride and bromide diffraction patterns. (d, e) TEM and HRTEM images of GaN synthesized in DOA using GaI_3 and $KGaBr_4$ salts, respectively.

chromatography−mass spectrometry (GC-MS) analysis of the $GaCl_3$−TOA product, which identified several decomposition products including chlorooctane and various alkenes and amines, including octylamine (Figure 1c and Supporting Information).

To explain the formation of species observed during thermal decomposition of TOA in the presence of GaX_3, we propose that terminal alkenes are formed via a Hofmann-type elimination of TOA bound to Lewis-acidic GaX_3. The decomposition of organics in the presence of reactive metal centers is well-documented.[27,28] The elevated temperatures in the presence of metal centers are expected to promote Hofmann elimination, yielding primary and secondary amines, ammonia, and terminal alkenes.[29,30] The terminal alkenes can also undergo metal-catalyzed isomerization to internal alkenes, a transformation well-documented in other metal systems.[31,32] The formation of longer alkyl chain compounds is also expected, as polymerization of 1-octadecene is known to occur during nanocrystal synthesis.[33] Similarly, our isomerized alkenes may also undergo polymerization. The detection of haloalkanes could indicate halogen reductive elimination or result from the reaction of metal halides with TOA, producing hydrogen halides that subsequently halogenate alkenes. Although reductive elimination is generally considered unlikely when electronegative heteroatoms such as nitrogen are bound to the metal center, our reactions are carried out at 300 °C, which may be sufficient to overcome these energetic barriers.[34] The behavior of aluminum chloride further supports the plausibility of a β-hydride elimination pathway: despite their limited redox activity, aluminum halides have been reported to break down polyethylene through hydride abstraction, β-scission, isomerization, and hydride transfer.[31,35]

Next, we sought to identify the difference in reactivity of InX_3 and GaX_3 halides toward alkylamines. The key distinction between $InCl_3$ and $GaCl_3$ in the presence TOA at 290 °C is that $GaCl_3$ generates substantially larger quantities of chloroalkanes, as outlined in Table S1. Given our insights from the GC−MS data (Figure 1c,d), we surmise that chloroalkane formation is the plausible reaction pathway that prevents synthesis of crystalline, phase pure Ga−pnictide nanocrystals. This decomposition route likely proceeds through covalent Ga−NR_2 intermediates, which are difficult to reverse because GaN has a large negative enthalpy of formation ($\Delta Hf^\circ = -156.8$ kJ mol^{-1}).[36] As a result, Ga−amide species become a thermodynamic sink that stalls further Ga−pnictide growth and leads to the formation of amorphous or highly defective nanocrystals. In contrast, transient In−amide species do not pose the same barrier: the ΔHf° of InN is less negative than that of InP or InAs (Table S2), so their formation does not kinetically stall the system. Moreover, colloidal synthesis of In−pnictides remains viable because a significant fraction of In−Cl bonds remain, allowing reaction with pnictide precursors even when partial amine decomposition occurs.

Collectively, these results suggest that the primary barrier to colloidal synthesis of gallium pnictides lies in their incompatibility with commonly used carboxylate precursors and alkylamine ligands that show strong tendency to form stable, unreactive byproducts.

Biphasic Approach to Synthesis of GaN Nanocrystals

To synthesize GaN nanocrystals, our group previously developed a biphasic reaction system, as shown in Figure 1a, using molten gallium halide salts in mixtures of TOA and HDA.[20] Maintaining an undissolved fraction of the gallium halide salt (i.e., preserving the biphasic nature of the system)

https://doi.org/10.1021/acs.chemmater.5c03186
Chem. Mater. XXXX, XXX, XXX−XXX

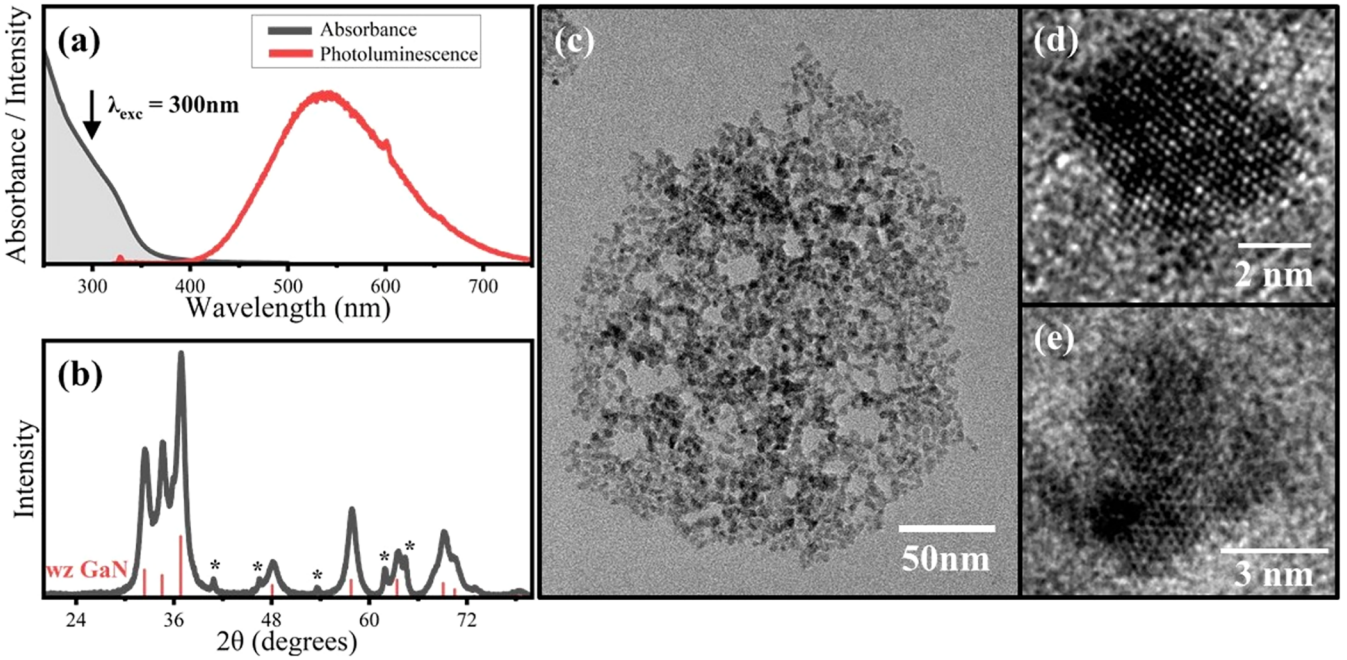

Figure 4. GaF_3-mediated synthesis of GaN nanocrystals in a mixture of trioctylamine and hexadecylamine. (a) Absorbance and photoluminescence spectra of GaN synthesized with 2 mol % GaF_3 (relative to GaI_3) salt added to the GaI_3 biphasic synthesis. (b) PXRD of the obtained GaN sample. Asterisks denote impurities that could not be removed. (c) TEM image of the colloidal GaN nanocrystals and (d, e) HRTEM images of colloidal GaN nanocrystals made by incorporating GaF_3 salt.

was found to be critical for successful GaN formation, typically requiring a gallium salt concentration of ~1.0 M. Most likely, the nucleation of GaN occurs in molten gallium halide salt droplets. A typical synthesis involves heating 5 mmol of gallium iodide (GaI_3) in 4 mL of TOA and 1 mL of HDA under a dry ammonia atmosphere at 290 °C for 1 h. To investigate the role of organic amines in this synthesis, we conducted modified biphasic reactions using pure primary (HDA), secondary (di-*n*-octylamine, DOA), and tertiary (TOA) amines, as outlined in Figure 2a. These reactions revealed significant differences between the resulting GaN nanocrystals. Powder X-ray diffraction (PXRD) analysis (Figure 2b) showed that reactions using pure TOA produced GaN with poor crystallinity, whereas both HDA and DOA yielded more crystalline products. To confirm the necessity of organic amines, a control reaction was conducted in hexadecane, which produced no crystalline GaN, underscoring the essential role of coordinating ligands in this biphasic system.

In addition to the critical role played by organic amines, the identity of the gallium halide precursor strongly influences GaN polytypism and particle morphology. PXRD patterns show that chloride and bromide precursors yield the wurtzite phase, as indicated by the (1011) reflection (reference line 1, Figure 3c), whereas the iodide precursor produces zinc blende GaN, identified by the zb (002) reflection at ~40° (reference line 2, Figure 3c). These structural differences are mirrored in the particle morphologies observed by TEM. GaN synthesized from chloride or bromide precursors form nanorods, consistent with anisotropic growth along the wurtzite *c*-axis and the sharp elongation of the (002) reflection in the PXRD patterns at 34.5° (Figures 3d and S3). For bromide-derived samples, the nanorods have an average length of 27 ± 8 nm and a diameter of 2.7 ± 0.5 nm (Figure S4a). In contrast, GaN derived from GaI_3 forms faceted, spheroidal nanocrystals with zinc blende symmetry and an average diameter of 3.3 ± 0.7 nm (Figures 3e and S4b).

This divergence in crystal structure can be rationalized in terms of anion size and effective ionicity effects, which have been shown to govern zinc blende−wurtzite stability in tetrahedrally coordinated semiconductors.[37] In nanocrystals, surface energetics play a dominant role in phase selection,[38] and the large, weakly electronegative iodide ion is expected to substantially modify surface composition and bonding.[38] Relative to chloride or bromide, iodide introduces a larger orbital radius and reduced surface ionicity, conditions that favor zinc blende stacking over the polar wurtzite arrangement.[37] Moreover, halide-based ammonoacidic GaN growth is known to proceed through distinct chemical intermediates, which may further influence surface termination and phase selection.[5] The observed differences in particle morphology are consistent with differences in halide−surface interactions. Chloride and bromide ions are expected to bind more strongly and selectively to GaN facets than iodide, given their higher bond dissociation energies,[39] enabling facet-selective growth that leads to rod-like morphologies. In contrast, the weaker and less selective binding of iodide is expected to reduce facet anisotropy, enabling more isotropic growth, resulting in the formation of zinc blende quantum dots.

We further explored phase control by partially substituting GaI_3 with GaF_3 in the biphasic reaction outlined in Figure 1a. Fluoride ions, owing to their small ionic radius and high electronegativity, are expected to coordinate more strongly to gallium centers than other halides, potentially stabilizing polar wurtzite surface terminations even in the absence of strongly anisotropic growth. In a modified version of the biphasic synthesis, approximately 2% of the GaI_3 precursor was replaced with GaF_3 (Figures 4 and S5). This minor compositional change led to the formation of significantly larger, nearly spherical GaN nanocrystals adopting the wurtzite structure

https://doi.org/10.1021/acs.chemmater.5c03186
Chem. Mater. XXXX, XXX, XXX−XXX

(Figure 4). The pronounced influence of fluoride is likely related to its strong coordination to gallium and its ability to substantially modify surface energetics during nanocrystal growth. This behavior is consistent with trends observed in ammonothermal GaN synthesis, where ammonium fluoride markedly accelerates crystal growth and stabilizes the wurtzite phase relative to chloride-, bromide-, or iodide-based mineralizers.[40] GaN synthesized with GaF_3 has an average diameter of 5.0 ± 1.2 nm compared to just 3.3 ± 0.7 nm in the pure iodide synthesis (Figure S4b,c). Taken together, these results demonstrate that GaN phase selection is governed by a delicate interplay between precursor speciation, halide identity, and surface chemistry, enabling deliberate tuning of nanocrystal structure through targeted modification of the halide environment.

To better understand the effect of organic amines, we utilized ^{1}H NMR spectroscopy to study the interactions between the various amines and gallium chloride ($GaCl_3$) salts (Figure S6). At a 1:3 Ga-to-amine molar ratio in deuterated benzene, TOA exhibited only weak coordination to gallium metal centers, as evident by the broadened α-proton signal, resulting from the rapid chemical exchange between bound and unbound TOA. In contrast, both HDA and DOA formed significantly stronger covalent interactions, displacing halide ligands. This was most evident with DOA, where the N−H proton signal observable at approximately 0.41 ppm disappeared at stoichiometric ratios, indicating the loss of the proton and formation of Ga-nitrogen bonds. HDA-$GaCl_3$ mixtures formed a dense, polymeric species poorly soluble in deuterated chloroform (Figure S7). Additionally, the downfield shifts of the α-protons in both HDA and DOA further confirmed the formation of robust covalent interactions with the gallium center. These downfield ^{1}H NMR shifts are expected for α-protons neighboring the gallium atom due to the deshielding effect of the gallium metal center.[41] To summarize, secondary amines have been shown to be highly effective for synthesizing crystalline GaN, while tertiary amines primarily serve as solvents and primary amines tend to form polymeric species that are not as conducive to crystalline GaN synthesis.

Given the improved crystallinity observed by PXRD for GaN synthesized using DOA compared to other amines, this system, employing GaI_3 as the gallium precursor under flowing ammonia at 270 °C, was selected for more comprehensive characterization. Under these conditions, approximately 3 nm GaN tetrahedral nanocrystals were obtained, as shown in Figure 3e. The absorbance spectrum of these nanocrystals exhibited a significant blue shift of the absorption edge relative to the bulk bandgap of zinc blende GaN (3.27 eV, 379 nm),[42] indicative of strong quantum confinement (Figure S8). However, photoluminescence (PL) measurements revealed only broad blue-green trap-state emission (Figure S8). This emission was confirmed to originate from the GaN nanocrystals via photoluminescence excitation (PLE) spectroscopy, which showed a direct correlation between the band edge absorbance and excitation spectra. The optical and structural properties of these GaN nanocrystals were comparable to those synthesized in biphasic reactions employing other amines.

The absence of band-edge PL may be suggestive of poor surface passivation, which is commonly observed in III−V quantum dots and often responsible for nonradiative recombination pathways. Fluoride treatments have proven highly effective for enhancing PL in related III−V systems such as InP[43] and InAs[44] nanocrystals. Motivated by these prior successes, we introduced a fluoride source directly into the reaction mixture to promote intrinsic optical emission. However, band-edge PL remained undetectable despite improved crystal growth. The emission instead consisted of broad trap-state PL, an optical signature that continues to dominate GaN samples synthesized via biphasic methods. These results suggest that while fluoride incorporation influences nanocrystal growth kinetics and morphology, surface trap states may not be the dominating factor for quenched band edge PL. Instead, internal defects may dominate trapping, requiring further strategies to achieve the quality necessary for bright band-edge emission in colloidal GaN quantum dots.

Having established the critical role of organic amines in the biphasic synthesis of GaN, we also investigated the role of ammonia in this process. Our findings show that both ammonia and organic alkyl amines are essential for the successful low-temperature formation of crystalline GaN phase. By selectively omitting components from the reaction, we gained important mechanistic insights into nitride formation. Notably, when ammonia was introduced via continuous flow to room temperature GaI_3 in the absence of alkyl amines, a strong interaction occurred, accompanied by a visible color change from lemon-yellow to white (Figure 5a−c). This

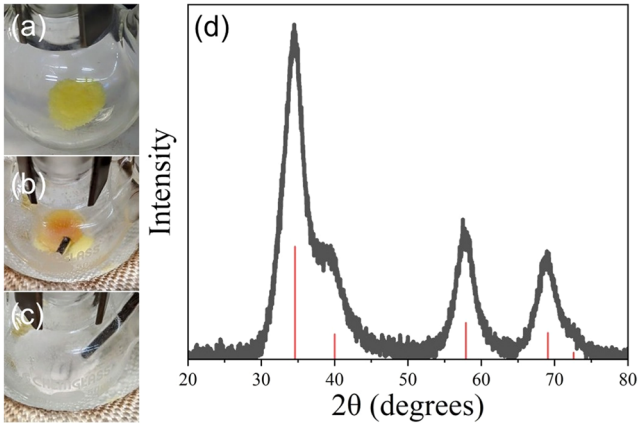

Figure 5. Role of gallium ammoniates in the biphasic GaN synthesis. (a−c) The evolution of GaI_3 powder placed under ammonia atmosphere, leading to the formation of gallium iodide ammoniates: (a) pure GaI_3; (b) exothermic reaction intermediate; and (c) final gallium iodide ammoniate. (d) PXRD of GaN nanocrystals synthesized by adding 4 mL TOA and 1 mL HDA to 5 mmol GaI_3 prereacted with ammonia (shown in panel c).

transformation indicates that ammonia readily coordinates with GaI_3. The reaction appeared to be exothermic, leading to melting of the GaI_3. After 5 min of ammonia exposure, a white powder remained in the reaction flask, with no visible evidence of the original GaI_3. However, no GaN was observed at this stage, as evidenced from the pure white coloration of the powder and the unique PXRD pattern obtained for this sample, which did not match GaN (Figure S9). When this gallium ammoniate complex was subsequently combined with an HDA−TOA organic amine mixture and heated to 290 °C under a nitrogen atmosphere, GaN nanocrystals were successfully synthesized. The resulting product exhibited a zinc blende crystal structure with an approximate Scherrer size

https://doi.org/10.1021/acs.chemmater.5c03186
Chem. Mater. XXXX, XXX, XXX−XXX

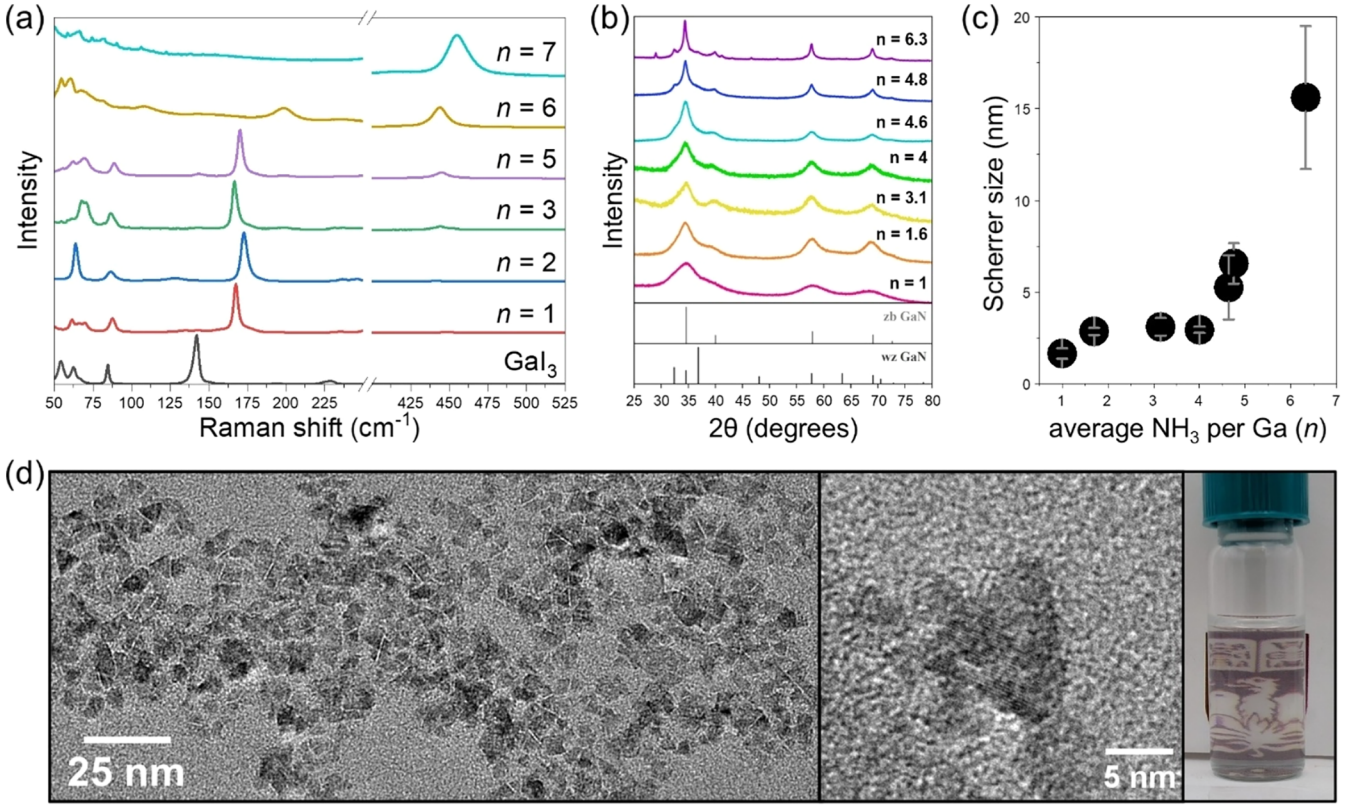

Figure 6. Gallium iodide ammoniates enable tunable synthesis of GaN nanocrystals. (a) A library of Raman spectra showing unique gallium iodide ammoniates with the formula $GaI_3 \cdot nNH_3$, where n = 1−7. Spectral break is from 250 to 400 cm^{-1}. (b) PXRD spectra of GaN synthesized by condensing a corresponding molar amount of ammonia (n) followed by adding 4 mL TOA and 1 mL HDA and heating to 290 °C for 1 h, reaction outlined in Figure 1b. (c) Scherrer size analysis of GaN synthesized using varying amounts of ammonia in our biphasic synthesis of GaN. (d) TEM images of GaN synthesized at 290 °C for 1 h using a mixture of $GaI_3 \cdot 7NH_3$ and $GaI_3 \cdot NH_3$ ammoniates (average n = 5), GaI_3 dissolved in DOA and TOA as the reaction solvents, reaction as outlines in Figure 1c. Left panel is a zoomed-out image showing overall particle morphology and shape. Middle panel is a high-resolution TEM showing lattice fringes on a tetrahedral, zinc-blende GaN nanocrystal. Right panel is a photograph of a solution of colloidal GaN nanocrystals synthesized using ammoniates and used for optical measurements. The image highlights the colloidal stability of the synthesized GaN nanocrystals evident by the clear transparent solution.

of 3.5 nm and was comparable in quality to GaN produced using our previously reported biphasic method (Figure 5d).[20]

Synthesis of GaN Nanocrystals Using Different Gallium Ammoniates

The coordination of ammonia to gallium halide salts is well-documented in bulk GaN synthesis,[6,45] though its role in colloidal nanomaterial synthesis remains unexplored. Since the reaction between GaI_3 and NH_3 is expected to produce gallium ammoniates,[46−49] the in situ formation of gallium ammoniate intermediates may play a key role in enabling GaN nanocrystal synthesis in biphasic systems. Overall, ammoniates are structurally analogous to hydrate salts, with ammonia instead of water as the coordinating ligand. A gallium heptaammoniate ($GaI_3 \cdot 7NH_3$) has been identified as an intermediate in the ammonothermal synthesis of bulk GaN under ammonoacidic conditions in supercritical ammonia.[46] Studies on ammonia's interaction with gallium halides date back to the 1930s, when hexammoniate complexes of $GaBr_3$ and GaI_3 were first reported after dissolving these salts in liquid ammonia at −33.5 °C.[47] Additionally, a monoammoniate species (i.e, $GaI_3 \cdot NH_3$) has been employed as a single-source precursor for the chemical vapor deposition (CVD) growth of GaN thin films.[50,51] In this study, we investigated the interaction between ammonia and GaI_3 by exposing GaI_3 to a continuous ammonia flow for up to 20 min at room temperature. Weight analysis revealed a stoichiometric ratio of GaI_3 to NH_3 of 1:4, suggesting that, on average, four ammonia molecules coordinate to the gallium metal center. This differs from the $GaI_3 \cdot 7NH_3$ complex observed under ammonothermal conditions, likely due to differences in reaction temperature, ammonia pressure, and ammonia concentration. However, a comprehensive library of aluminum halide ammoniates ($AlX_3 \cdot nNH_3$, n = 1, 2, 3, 5, 6, 7, where n = 4 was reported not to be observable) has been previously synthesized and characterized via single-crystal XRD.[52] Given the chemical similarities between aluminum and gallium halides, analogous structures between the two systems are expected.

To further investigate the role of ammoniates in the reaction, we tuned the ammonia-to-gallium ratio by dosing GaI_3 with controlled amounts of ammonia gas (see Methods section). This approach enabled the preparation of a series of $GaI_3 \cdot nNH_3$ complexes (n = 1, 2, 3, 5, 6, 7), each displaying a distinct Raman spectrum (Figure 6a). Pristine GaI_3 exhibits a dominant Raman band at 142 cm^{-1} with weaker features below 100 cm^{-1}, consistent with Ga−I stretching and bending modes reported in the literature. Low-order ammoniates ($GaI_3 \cdot 1NH_3$ to $GaI_3 \cdot 5NH_3$) retain this primary dominant mode, which shifts to ∼170 cm^{-1}, indicating initial perturbation of the Ga−I symmetry upon ammonia coordination. Differences among these species are most evident in the additional vibrational

https://doi.org/10.1021/acs.chemmater.5c03186
Chem. Mater. XXXX, XXX, XXX−XXX

features appearing between 50 and 100 cm^{-1}. At higher ammonia loadings ($GaI_3 \cdot 6NH_3$ and $GaI_3 \cdot 7NH_3$), the characteristic Ga−I lattice mode disappears entirely, consistent with complete ammonia coordination to gallium and displacement of iodide into the outer coordination sphere. Concurrently, Raman bands emerge near 440−460 cm^{-1}, which are absent GaI_3 and weak in low-order ammoniates. The Raman spectrum of $GaI_3 \cdot 7NH_3$ matches previously reported data and was verified by direct comparison.[46] Lastly, $GaI_3 \cdot 4NH_3$ could not be isolated under these conditions (Figure S10), consistent with prior reports showing that analogous aluminum halide−ammonia complex of this stoichiometry was similarly unobservable.[52]

Gaining insight into the formation of gallium ammoniate intermediates marked a step forward in understanding the mechanism of GaN nanocrystal synthesis. Importantly, these intermediates can be directly incorporated into the biphasic reaction, eliminating the need to inject large quantities of difficult-to-dry and corrosive ammonia gas. Our initial results revealed that the size of GaN nanocrystals can be tuned simply by varying the ammoniate order (n) in $GaI_3 \cdot nNH_3$, which denotes the average number of ammonia molecules coordinated to GaI_3 (Figure 6b,c). By using a pressure reaction vessel, as illustrated in Figure S11a, a known pressure of ammonia could be condensed onto gallium iodide powder using a dry ice-acetone bath. Once all the ammonia had condensed, the ammoniate mixture was then heated (150 °C−300 °C) to homogenize the ammoniate order. By using this technique, we have been able to precisely control the amount of ammonia present in our biphasic reactions. Figure 6c demonstrates that after adding organic amines and heating the slurry of ammoniates to 290 °C under nitrogen, the size of GaN nanocrystals synthesized could be tuned by varying the amount of ammonia coordinated to gallium. However, we should note that this method resulted in poor homogeneity, as the ammoniate would sublime out of the bottom hot zone and condense on the upper cold zone side walls. Therefore, in order to build the ammoniate library found in Figure 6a, unhomogenized powders were sealed inside a quartz ampule and heated to 200 °C for 24 h, which resulted in more pure ammoniate samples.

Using our library of gallium ammoniates, we sought to investigate the mechanistic role of these ammoniates in GaN formation. For this, we first compared two extremes: $GaI_3 \cdot 1NH_3$ and $GaI_3 \cdot 7NH_3$. Notably distinct results were obtained (Supporting Figure S12). As expected, based on our initial size tunability results with GaI_3 precursor, the limited Ga−NH_3 stoichiometry for the monoammoniate ($GaI_3 \cdot 1NH_3$) produced small zinc blende GaN nanocrystals, with Scherrer sizes below 2.4 nm. More unexpectedly, the heptaammoniate, $GaI_3 \cdot 7NH_3$ heated to 290 °C in TOA produced a largely amorphous material with a mostly featureless PXRD pattern, bearing a resemblance to polymeric gallium imide (Figure S13). Raman analysis of this product showed no resemblance to any known ammoniate species but found Raman features characteristic of Ga−I bonds (Figure S14), suggesting the very high thermal stability of $GaI_3 \cdot 7NH_3$, which was apparently detrimental for nucleation of GaN nanocrystals. The enhanced stability of ammoniates with n = 6, 7 can be explained by the hard and soft acid and base (HSAB) principle. Generally, Ga(III), which is a hard Lewis acid, is expected to bind more strongly with hard Lewis bases like NH_3 rather than with soft I^-. The least favorable scenario occurs when the metal is coordinated with mixed hard and soft ligands, leading to the reduced stability and faster ligand exchange kinetics. This HSAB mismatch naturally occurs in $GaI_3 \cdot nNH_3$ for n = 1, whereas in higher ammoniates, the coordination of Ga(III) is composed of strongly bonded NH_3 ligands as evidenced by the disappearance of the Raman peaks around 170 cm^{-1} associated with Ga−I bonds (Figure 6a).

We propose that unstable lower-order ammoniates promote GaN nucleation, while higher-order ammoniates are less reactive and primarily contribute to the nanocrystal growth. To probe the relationship between ammoniate composition and nanocrystal growth more deeply, a mixed precursor approach was employed. A 4:1 molar ratio of $GaI_3 \cdot 7NH_3$ to $GaI_3 \cdot 1NH_3$ was used in the reaction. Under these conditions, significantly larger GaN nanocrystals (∼5 nm) were obtained (Figure S12), demonstrating that controlled ammoniate loading can balance reactivity and crystal growth, leading to size-tunable GaN formation. This result is consistent with the trend observed in Figure 5c, where increasing the average ammonia content led to larger nanocrystals. To determine whether ammoniate mixtures equilibrate upon heating, we compared two reactions with equivalent average ammonia loading (n = 5): one using pure $GaI_3 \cdot 5NH_3$ and the other a mixture of $GaI_3 \cdot 7NH_3$ and $GaI_3 \cdot 1NH_3$. The mixed system yielded GaN nanocrystals with an average Scherrer size over 40% larger (Figure S15), suggesting that ammoniate speciation—not just total ammonia content—plays a key role in determining nanocrystal size.

In colloidal syntheses using GaI_3 as the gallium source, we found that nanocrystals smaller than ∼5 nm consistently adopted the zinc blende structure, as revealed by PXRD. However, once the nanocrystal size exceeded this threshold, reflections corresponding to the wurtzite phase began to emerge alongside the dominant zinc blende peaks (Figures 6b, and S16), indicating the appearance of wurtzite domains, often associated with the accumulation of stacking faults during crystal growth. TEM analysis of these larger GaN nanocrystals (Figure S17a,b) revealed significant heterogeneity in both size and morphology, with prominent faceting and irregular shapes having an average size of 6.4 ± 2.3 nm with an overall size dispersion of 35%. This was in contrast to reactions conducted using GaI_3 under continuous ammonia flow which had size dispersion of less than 25%. While continuous ammonia flow could only produce nanocrystals of one size, they were more uniform particles, suggesting that dynamic precursor speciation plays a role in structural evolution. To probe this effect, we implemented a modified synthesis in which 1 mmol of GaI_3 was predissolved in 1 mL of DOA prior to the addition of gallium ammoniate powder (0.8 mmol $GaI_3 \cdot NH_3$ and 3.2 mmol $GaI_3 \cdot 7NH_3$) and 4 mL of TOA. Under these conditions, PXRD analysis showed complete suppression of the wurtzite phase (Figure S16), and TEM images (Figures 6d and S17c) revealed tetrahedral nanocrystals of 4.6 ± 1.0 nm diameter and size dispersion of 21%, consistent with what had been observed under continuous ammonia flow. This result supports the idea that controlling the early coordination environment of gallium precursors can stabilize the zinc blende phase and preventing nonuniform growth, presumably by minimizing stacking fault formation during nucleation and growth.

■ CONCLUSIONS

This work establishes a framework for the tunable synthesis of GaN nanocrystals via biphasic molten salt/organic solvent

https://doi.org/10.1021/acs.chemmater.5c03186
Chem. Mater. XXXX, XXX, XXX−XXX

reactions, highlighting the important roles of halide ions, organic amines and ammonia. Through a detailed study of gallium halide-ammonia interactions, we identify gallium ammoniate intermediates as key precursors that enable GaN formation under mild conditions, establishing the existence of a library of ammoniate precursors. We demonstrate that the ammoniate order (i.e., the amount of coordinated ammonia) governs both the reactivity and final nanocrystal size, with low-order ammoniates promoting nucleation and high-order species facilitating growth. A mixed-ammoniate strategy allows more precise control over size and phase. Furthermore, comparative analysis of the indium and gallium halide systems underscores the unique challenges of GaN synthesis, which arise from the high thermal stability of catalytically derived gallium intermediates. These insights not only deepen our understanding of III−V nanocrystal formation but also pave the way for more efficient, tunable routes to GaN and other challenging semiconductor materials. As the next step toward the colloidal synthesis of GaN quantum dots with bright band edge emission, we may need to learn from the recent studies on GaAs nanocrystals, highlighting the difficulty with defect-free crystallization of gallium-based pnictides without applying high temperatures typically associated with CVD rather than colloidal syntheses, which requires approaches alternative to organic-phase colloidal synthesis.[53,54]

METHODS

Chemicals

Acetonitrile (Sigma-Aldrich, anhydrous, 99.8%), ammonia gas (Airgas, anhydrous grade), Benzene-d_6 (Cambridge Isotope Laboratories, D, 99.96%), chloroform-*d* ($CDCl_3$, Sigma-Aldrich, 99.8 atom % D), cyclohexane (Sigma-Aldrich, anhydrous, 99.5%), di-n-octylamine (DOA, TCI, >96.0%), ethanol (Sigma-Aldrich, ≥99.5%, anhydrous), gallium metal (Thermo Fisher, 99.999%), gallium(III) chloride ($GaCl_3$, Strem, anhydrous, granular, 99.999%-Ga, PURATREM), hexadecane (Sigma-Aldrich, ReagentPlus, 99%), hexadecylamine (HDA, Sigma-Aldrich, technical grade, 90%), indium(III) chloride ($InCl_3$, Strem, anhydrous, 99.999%-In, PURATREM), iodine (Sigma-Aldrich, ReagentPlus, ≥99.8%), methanol (Sigma-Aldrich, 99.8%, anhydrous), methylcyclohexane (MCH, Sigma-Aldrich, anhydrous, ≥99%), 1-octene (Sigma-Aldrich, 98%), oleic acid (OA, Sigma-Aldrich, technical grade, 90%), oleylamine (OAm, Sigma-Aldrich, technical grade, 70%), palmitic acid (PA, Sigma-Aldrich, ≥99%), toluene (Sigma-Aldrich, anhydrous, 99.8%), tri-*n*-octylamine (TOA, Sigma-Aldrich, 98%) were used as received from the supplier except as noted below.

OAm, TOA, HDA, and DOA were vacuum distilled over sodium metal (Sigma-Aldrich, in kerosene, pieces, ≥99.8%) and stored in a nitrogen filled glovebox; the liquids were stored over dried 4 Å molecular sieves. Ammonia gas was further purified by passing through a gas purifier (Entergris, MC1−702F) or by condensation over sodium metal. PA was dried under vacuum overnight. Hexadecane was dried by degassing under vacuum at 100 °C for 3 h.

Safety Considerations

Pressurized glass vessels and ampules pose a risk of explosive rupture. Proper shielding must always be used, and each vessel should be carefully inspected for cracks, scratches, or other defects before use; any compromised vessels must be discarded. Additionally, O-ring materials must be compatible with ammonia. Neoprene and Buna-N are suitable choices, whereas fluoroelastomers such as Viton are not compatible and should be avoided.

Synthesis of Gallium Iodide

To begin, iodine was dried by subliming through 4 Å molecular sieves as described by a previous method.[55,56] Here, the iodine was collected in a reaction flask with a removable top to more easily remove iodine. The dried iodine was stored in a nitrogen filled glovebox and kept in a Ziploc plastic bag to prevent diffusion of iodine vapor throughout the glovebox, which can contaminate surfaces and poison the copper catalyst. Before handling iodine, it was first cooled in a freezer or cold trap (cooled by liquid nitrogen) to reduce the vapor pressure of the elemental iodine (i.e., no purple vapor was observed in the container headspace).

Next, molten Ga metal (approximately 50 °C) and small chunks of dried iodine were combined in a one-inch quartz ampule at a 1:3/2 Ga-to-I_2 molar ratio (first cooled in our glovebox cold trap to prevent release of iodine vapor). Typical reaction scale was approximately 100 g.

Finally, the quartz ampule was flame-sealed under vacuum using methods previously described. (Note that the iodine and Ga in the ampule were placed in liquid nitrogen to prevent any losses during vacuum flame sealing of the ampule). The ampule was then placed in a rocking furnace which was first heated to 180 °C to melt the elements and initiate the reaction. After 1 h at 180 °C, the reaction temperature was increased to 220 °C to melt the formed GaI_3 and allow the reaction to continue. After another hour, the temperature was increased to 300 °C for 12 h to ensure complete reaction of all iodine and gallium. *Caution!* This multistage heating process is crucial to prevent overpressurization of the ampule, which can shatter it to release I_2 vapor.

The synthesized GaI_3 was removed from the quartz ampule in a nitrogen-filled glovebox and transferred into a sublimator (Chemglass, CG-3038). To open the ampule, a scribing tool was used to make 4 lines up and down the ampule, then a glass tube cutter was used to etch sections into the ampule, and finally the ampule was gently hit with a pestle to break the glass ampule apart and recover the gallium iodide. This process was done over a plastic bag or wax paper to catch any GaI_3 pieces and prevent them from becoming contaminated on the glovebox floor. Note that metal foil should not be used, as it will quickly alloy with gallium iodide. The gallium iodide was sublimed at 140 °C under dynamic vacuum by placing the sublimator in a beaker heating mantle (Glas-Col, 100A O610). The temperature is important to ensure that no gallium oxide species sublime with the gallium iodide.[57] The sublimator cold trap was filled with acetone to maintain the coldfinger at sufficiently low temperature to collect the sublimed GaI_3. The sublimation was left to run overnight, typically taking more than 10 h to complete. The recovered gallium iodide was stored in amber glass vials in a nitrogen-filled glovebox.

Synthesis of $GaI_3{\cdot}nNH_3$ (n = 1−6) Ammoniates

Gallium iodide (GaI_3) was weighed into a 3 oz glass pressure reaction vessel (PRV, Astraglass Innovations, 1104520003) and sealed inside a nitrogen-filled glovebox using a needle valve adaptor (Astraglass, 1109570001). The sealed vessel was then transferred out of the glovebox and placed on a custom-built Schlenk line assembly, as shown in Figure S8. Once under nitrogen atmosphere, ammonia gas was introduced volumetrically to achieve the desired stoichiometric ratio for $GaI_3{\cdot}nNH_3$. That is, given a known mass of GaI_3, in a known volume, a specific pressure of ammonia could be applied (i.e., PV = nRT). The vessel was then sealed within 10 s to prevent excess ammonia uptake. The reaction commenced within 30−60 s, as indicated by an exothermic response and a pressure drop inside the PRV.

The sealed vessel was kept at room temperature for 30 min to allow the reaction to proceed, followed by submersion in a dry ice−acetone bath for an additional 30 min to ensure complete reaction. After returning to room temperature, the vessel was transferred back to the glovebox, and the resulting ammoniate was transferred to a quartz ampule. The ampule was then flame-sealed under liquid nitrogen and placed in a tube furnace at 220 °C (n = 1−3) or 300 °C (n = 4−6) for 24 h to ensure sample uniformity, based on aluminum ammoniate synthesis.[52,58,59]

As a note, while numerous transition metal ammoniate salts have been identified,[52] water preferentially binds over ammonia and readily displaces coordinated ammonia upon air exposure. This underscores the necessity of maintaining anhydrous, oxygen-free conditions during

https://doi.org/10.1021/acs.chemmater.5c03186
Chem. Mater. XXXX, XXX, XXX−XXX

GaN synthesis to prevent unwanted hydrolysis and the formation of gallium oxynitrides.

Synthesis of $GaI_3 \cdot 7NH_3$ Ammoniate

GaI_3 was loaded into a glass PRV inside a nitrogen-filled glovebox. The sealed vessel was transferred to the home-built Schlenk line and placed under nitrogen using standard air-free handling techniques. Excess ammonia was then condensed onto the GaI_3 by submerging the PRV in liquid nitrogen, a more efficient method than using a dry ice−acetone bath. Once a sufficient amount of ammonia had solidified, the vessel was sealed and allowed to warm to room temperature, where the ammonia melted and completely dissolved the GaI_3. The vessel was then slowly vented to remove all ammonia, which was passed through a copper sulfate solution to neutralize excess ammonia gas from release into the fume hood exhaust. The remaining product, a fluffy white powder, was flushed with nitrogen to remove residual ammonia gas. The $GaI_3 \cdot 7NH_3$ product was stored inside a nitrogen-filled glovebox, and its identity was confirmed via Raman spectroscopy.[46]

Synthesis of GaN Nanocrystals

GaN nanocrystals synthesized under continuous ammonia flow have been previously described and the procedure is outlined in Figure 1a.[20] Synthesis with DOA followed the same procedure as the original biphasic GaN synthesis, with the following modifications: Hexadecylamine (HDA) and trioctylamine (TOA) were replaced with 5 mL of di-*n*-octylamine (DOA). Additionally, the final reaction temperature was reduced from 290 to 270 °C. All purification and product isolation steps remained unchanged.

For the synthesis of GaN via the ammonia condensation method, outlined in Figure 1b, 5 mmol of GaI_3 was loaded into a glass pressure reaction vessel inside a nitrogen filled glovebox and sealed with a needle valve adaptor. A known amount of ammonia was then condensed onto the GaI_3 while the vessel was submerged in a dry ice acetone bath. The amount of ammonia was controlled by applying a measured pressure in a known volume and quickly sealing the reaction vessel. Once the measurable pressure had dropped to zero, the vessel was transferred back to the glovebox and 4 mL of TOA, 1 mL of HDA, and a glass stir bar were added. The vessel was transferred air-free to a Schlenk line and placed under nitrogen. The vessel was heated to 290 C for 1 h. Alternatively, the gallium ammoniate powder could be transferred to a round-bottom flask, but this took more time and it is challenging to get all of the ammoniate into the round-bottom flask.

To synthesize GaN using the controlled ammoniate method outlined in Figure 1c, 1 mmol of GaI_3, 1 mL of hexadecylamine (HDA) preheated to 75 °C, and 4 mL of trioctylamine (TOA) were combined in a 50 mL three-neck round-bottom flask equipped with a thermowell, stopcock adapter, and rubber septum inside a nitrogen filled glovebox. The flask was transferred under air-free conditions to a Schlenk line, placed under nitrogen, and heated to 100 °C until all GaI_3 dissolved, forming a uniform solution. The flask was then returned to the glovebox, and 4 mmol of gallium ammoniate powder was added (e.g., 375 mg GaI3·1NH_3 and 1.825 g GaI3·7NH_3). The reaction flask was subsequently transferred back to the Schlenk line under nitrogen. The reaction mixture was stirred vigorously to create a vortex without splashing, then heated to 290 °C. After 1 h, the heating mantle was removed, and the reaction was cooled to room temperature. The synthesized GaN was not initially colloidally stable, consistent with the products observed for all biphasic reactions.

Purification steps were carried out under nitrogen inside a glovebox. To clean the GaN nanocrystals, 10 mL of toluene was added to the reaction mixture and stirred to dissolve organic byproducts. The mixture was transferred to a 50 mL centrifuge tube and centrifuged. The supernatant was discarded, and 20 mL of anhydrous methanol was added to the precipitate, followed by vortex agitation to suspend the product and dissolve ammonium iodide byproducts. The mixture was then centrifuged to precipitate the GaN product.

For colloidal stabilization, the precipitate was resuspended in 10 mL of anhydrous cyclohexane (or methylcyclohexane) with 200 mg of degassed palmitic acid (PA) or oleic acid (OA). The centrifuge tube was sealed with electrical tape to prevent leaks. Outside the glovebox, the mixture was briefly sonicated (≤1 min) to promote colloidal stabilization, forming a transparent pale-yellow solution. To remove insoluble impurities, the solution was centrifuged, and the supernatant was collected. Ethanol was added to induce nanocrystal flocculation, followed by centrifugation to precipitate the particles. The washing step with ethanol was repeated twice to remove excess palmitic acid. The final purified nanocrystals were suspended in 8 mL of anhydrous cyclohexane or methylcyclohexane.

Characterization

TEM images were obtained with a 300 kV FEI Tecnai G2 F30 microscope or a 200 kV Tecnai F20 microscope. Absorption spectra of solution samples were acquired using a Shimadzu UV-3600 Plus spectrophotometer from 200 to 700 nm. Photoluminescence (PL) and photoluminescence excitation (PLE) spectra of solution samples were acquired with a Horiba FluoroMax-4. PXRD patterns were obtained with a Rigaku MiniFlex with a Cu Kα source, with samples drop-cast onto a silicon zero background sample holder. Raman measurements were performed using a HORIBA LabRAM HR Evolution Confocal Raman Microscope. Raman samples were drop-cast onto or (for powders) placed under a glass substrate encapsulation coverslip and sealed onto a glass microscope slide using ultraviolet-curing epoxy resin to protect the sample from air exposure. All Raman samples were prepared in a nitrogen-filled glovebox. GC-MS data was collected on an Agilent Tech HP-5 Å MS (electron ionization source, 30 m × 0.25 mm × 0.25 μM column) with an Agilent 5975 Series MSD, Hewlett-Packard 7683 Series injector and Agilent 6890 series GC instrument. Samples were prepared by reacting 1 mmol metal halide salt with 3 mmol of distilled TOA at 290 °C for 1 h. The samples were then diluted with anhydrous acetonitrile in a glovebox to a concentration of 5 mg/mL based on the metal halide salt, and a 1 mL aliquot was added to a screw-cap GC vial for analysis.

■ ASSOCIATED CONTENT

Supporting Information

The Supporting Information is available free of charge at https://pubs.acs.org/doi/10.1021/acs.chemmater.5c03186.

Additional experimental details; ^{1}H and ^{13}C NMR spectra of gallium halide/solvent reactions and octene byproduct identification; GC-MS analysis of trioctylamine degradation; thermodynamic data tables; TEM images and size histograms of GaN nanocrystals; PXRD data for GaN products, ammoniate-derived samples, and phase comparisons; absorbance, PL, and PLE spectra; Raman spectra of gallium ammoniates, gallium salts, and amine−gallium halide mixtures; photographs of gallium iodide ammoniates, their synthesis vessel, and air-stability behavior (Figures S1−S17 and Tables S1 and S2) (PDF)

GC-MS Data Readout (PDF)

■ AUTHOR INFORMATION

Corresponding Author

Dmitri V. Talapin − *Department of Chemistry, University of Chicago, Chicago, Illinois 60637, United States; James Franck Institute and Pritzker School of Molecular Engineering, University of Chicago, Chicago, Illinois 60637, United States; Center for Nanoscale Materials, Argonne National Laboratory, Lemont, Illinois 60439, United States;* orcid.org/0000-0002-6414-8587; Email: dvtalapin@uchicago.edu

https://doi.org/10.1021/acs.chemmater.5c03186
Chem. Mater. XXXX, XXX, XXX−XXX

Authors

James Cassidy − *Department of Chemistry, University of Chicago, Chicago, Illinois 60637, United States; James Franck Institute, University of Chicago, Chicago, Illinois 60637, United States;* orcid.org/0009-0009-6719-4245

Ruiming Lin − *James Franck Institute and Pritzker School of Molecular Engineering, University of Chicago, Chicago, Illinois 60637, United States;* orcid.org/0000-0002-6750-0566

Alexandra Krupinski − *Department of Chemistry, University of Chicago, Chicago, Illinois 60637, United States*

Maia Czaikowski − *Department of Chemistry, University of Chicago, Chicago, Illinois 60637, United States;* orcid.org/0000-0002-1334-8140

Wooje Cho − *Department of Chemistry, University of Chicago, Chicago, Illinois 60637, United States; James Franck Institute, University of Chicago, Chicago, Illinois 60637, United States*

John S. Anderson − *Department of Chemistry, University of Chicago, Chicago, Illinois 60637, United States;* orcid.org/0000-0002-0730-3018

Complete contact information is available at: https://pubs.acs.org/10.1021/acs.chemmater.5c03186

Author Contributions

The manuscript was written through contributions of all authors. All authors have given approval to the final version of the manuscript.

Notes

The authors declare no competing financial interest.

■ ACKNOWLEDGMENTS

We thank Dr. A. Nelson for reading and editing the manuscript. We also thank Dr. J. Jureller and Dr. S. Brown for help with Raman measurements. The work on synthesis of GaN NCs was funded by the U.S. Department of Energy, Office of Science, Basic Energy Sciences, Materials Sciences and Engineering Division, under grant DE-SC0025256. Structural and spectroscopic characterizations of novel III−V quantum dots were supported by the National Science Foundation Science and Technology Center (STC) for Integration of Modern Optoelectronic Materials on Demand (IMOD) under Award No. DMR-2019444. This work made use of the shared facilities at the University of Chicago Materials Research Science and Engineering Center, supported by National Science Foundation under award number DMR-2011854. Parts of this work were carried out at the Soft Matter Characterization Facility of the University of Chicago. We also acknowledge support from the Samsung Advanced Institute of Technology (SAIT) through the Samsung QD Cluster Collaboration. Work performed at the Center for Nanoscale Materials, a U.S. Department of Energy Office of Science User Facility, was supported by the U.S. DOE, Office of Basic Energy Sciences, under Contract No. DE-AC02-06CH11357.

■ REFERENCES

(1) Arteev, D. S.; Sakharov, A. V.; Zavarin, E. E.; Lundin, W. V.; Smirnov, A. N.; Davydov, V. Y.; Yagovkina, M. A.; Usov, S. O.; Tsatsulnikov, A. F. Investigation of Statistical Broadening in InGaN Alloys. *J. Phys.: Conf. Ser.* **2018**, *1135* (1), No. 012050.

(2) Jewett, S. A.; Makowski, M. S.; Andrews, B.; Manfra, M. J.; Ivanisevic, A. Gallium Nitride Is Biocompatible and Non-Toxic before and after Functionalization with Peptides. *Acta Biomater.* **2012**, *8* (2), 728−733.

(3) de Rooij, M.; Pozo, A.; Colino, S.; Glaser, J.; Palma, M.; Wattenberg, M.; Zafrani, M.; Lidow, A.; Strittmatter, R.; Marini, T.; Durkin, S.; Honea, J.; Huang, A. Q.; Nazerian, E.; Han, P.; Di Paolo Emilio, M. Applications of GaN Technology. In *GaN Technology: Materials, Manufacturing, Devices and Design for Power Conversion*; Di Paolo Emilio, M., Ed.; Springer Nature: Switzerland: Cham, 2024; pp 111−183 DOI: 10.1007/978-3-031-63238-9_5.

(4) Griffiths, S.; Pimputkar, S.; Kearns, J.; Malkowski, T. F.; Doherty, M. F.; Speck, J. S.; Nakamura, S. Growth Kinetics of Basic Ammonothermal Gallium Nitride Crystals. *J. Cryst. Growth* **2018**, *501*, 74−80.

(5) *Ammonothermal Synthesis and Crystal Growth of Nitrides: Chemistry and Technology*; Meissner, E.; Niewa, R., Eds.; Springer Series in Materials Science; Springer International Publishing: Cham, 2021; Vol. *304* DOI: 10.1007/978-3-030-56305-9.

(6) Stoddard, N.; Pimputkar, S. Progress in Ammonothermal Crystal Growth of Gallium Nitride from 2017−2023: Process, Defects and Devices. *Crystals* **2023**, *13* (7), No. 1004.

(7) Hwang, J.-W.; Campbell, J. P.; Kozubowski, J.; Hanson, S. A.; Evans, J. F.; Gladfelter, W. L. Topochemical Control in the Solid-State Conversion of Cyclotrigallazane into Nanocrystalline Gallium Nitride. *Chem. Mater.* **1995**, *7* (3), 517−525.

(8) Janik, J. F.; Wells, R. L. Gallium Imide, {Ga(NH)3/2}n, a New Polymeric Precursor for Gallium Nitride Powders. *Chem. Mater.* **1996**, *8* (12), 2708−2711.

(9) Mićić, O. I.; Ahrenkiel, S. P.; Bertram, D.; Nozik, A. J. Synthesis, Structure, and Optical Properties of Colloidal GaN Quantum Dots. *Appl. Phys. Lett.* **1999**, *75* (4), 478−480.

(10) Pan, G.; Kordesch, M. E.; Van Patten, P. G. New Pyrolysis Route to GaN Quantum Dots. *Chem. Mater.* **2006**, *18* (17), 3915−3917.

(11) Sardar, K.; Rao, C. N. R. New Solvothermal Routes for GaN Nanocrystals. *Adv. Mater.* **2004**, *16* (5), 425−429.

(12) Choi, Y. C.; Kim, H.; Lee, C.; Son, J.; Baik, H.; Park, S.; Kim, J.; Jeong, K. S. Blue Emission of α-GaN Colloidal Quantum Dots via Zn Doping. *Chem. Mater.* **2019**, *31* (15), 5370−5375.

(13) Liao, S. M.; Wen, J. H.; Chou, W. C.; Lan, S. M. Photoluminescence Characterization of GaN Thin Film Grown by Atmospheric Pressure Organometallic Vapor Phase Epitaxy. *Mater. Sci. Eng.: B* **1997**, *48* (3), 205−210.

(14) Gaiser, H. F.; Popescu, R.; Gerthsen, D.; Feldmann, C. Ionic-Liquid-Based Synthesis of GaN Nanoparticles. *Chem. Commun.* **2020**, *56* (15), 2312−2315.

(15) Manz, A.; Birkner, A.; Kolbe, M.; Fischer, R. A. Solution Synthesis of Colloidal Gallium Nitride at Unprecedented Low Temperatures. *Adv. Mater.* **2000**, *12* (8), 569−573.

(16) Xie, Y.; Qian, Y.; Wang, W.; Zhang, S.; Zhang, Y. A Benzene-Thermal Synthetic Route to Nanocrystalline GaN. *Science* **1996**, *272* (5270), 1926−1927.

(17) Yu, L.; Lv, Y.; Zhang, X.; Zhao, Y.; Zhang, Y.; Huang, H.; Feng, Y. A Soluble Salt-Assisted Facile Synthetic Route to Semiconducting GaN Nanoparticles. *CrystEngComm* **2010**, *12* (7), 2037−2039.

(18) Reshchikov, M. A. Point Defects in GaN. In *Semiconductors and Semimetals*; Romano, L.; Privitera, V.; Jagadish, C., Eds.; Defects in Semiconductors; Elsevier, 2015; Chapter 9, Vol. *91*, pp 315−367 DOI: 10.1016/bs.semsem.2014.11.003.

(19) Soignard, E.; Machon, D.; McMillan, P. F.; Dong, J.; Xu, B.; Leinenweber, K. Spinel-Structured Gallium Oxynitride (Ga3O3N) Synthesis and Characterization: An Experimental and Theoretical Study. *Chem. Mater.* **2005**, *17* (22), 5465−5472.

(20) Cho, W.; Zhou, Z.; Lin, R.; Ondry, J. C.; Talapin, D. V. Synthesis of Colloidal GaN and AlN Nanocrystals in Biphasic Molten Salt/Organic Solvent Mixtures under High-Pressure Ammonia. *ACS Nano* **2023**, *17* (2), 1315−1326.

(21) Palomaki, P. K. B.; Miller, E. M.; Neale, N. R. Control of Plasmonic and Interband Transitions in Colloidal Indium Nitride Nanocrystals. *J. Am. Chem. Soc.* **2013**, *135* (38), 14142−14150.

(22) Wen, D.; Kirkwood, N.; Mulvaney, P. Synthesis of Size-Tunable Indium Nitride Nanocrystals. *J. Phys. Chem. Lett.* **2023**, *14* (15), 3669−3676.
(23) Karan, N. S.; Chen, Y.; Liu, Z.; Beaulac, R. Solution−Liquid−Solid Approach to Colloidal Indium Nitride Nanoparticles from Simple Alkylamide Precursors. *Chem. Mater.* **2016**, *28* (16), 5601−5605.
(24) Basel, S.; Bhardwaj, K.; Pradhan, S.; Pariyar, A.; Tamang, S. DBU-Catalyzed One-Pot Synthesis of Nearly Any Metal Salt of Fatty Acid (M-FA): A Library of Metal Precursors to Semiconductor Nanocrystal Synthesis. *ACS Omega* **2020**, *5* (12), 6666−6675.
(25) Gary, D. C.; Terban, M. W.; Billinge, S. J. L.; Cossairt, B. M. Two-Step Nucleation and Growth of InP Quantum Dots via Magic-Sized Cluster Intermediates. *Chem. Mater.* **2015**, *27* (4), 1432−1441.
(26) Kim, T.; Park, S.; Jeong, S. Diffusion Dynamics Controlled Colloidal Synthesis of Highly Monodisperse InAs Nanocrystals. *Nat. Commun.* **2021**, *12* (1), No. 3013.
(27) Karimzadeh-Younjali, M.; Wendt, O. F. α- and β-Eliminations in Transition Metal Complexes: Strategies to Cleave Unstrained C−C and C−F Bonds. *Helv. Chim. Acta* **2021**, *104* (11), No. e2100114.
(28) Buchan, N. I.; Yu, M. L. β-Hydride Elimination Reaction of Triethylgallium on GaAs(100) Surfaces. *Surf. Sci.* **1993**, *280* (3), 383−392.
(29) Cope, A. C.; Trumbull, E. R. Olefins from Amines: The Hofmann Elimination Reaction and Amine Oxide Pyrolysis. In *Organic Reactions*; John Wiley & Sons, Ltd, 2011; pp 317−493 DOI: 10.1002/0471264180.or011.05.
(30) Chen, H.; Abdelrahman, O. A. Cooperative Adsorption: Solvating the Hofmann Elimination of Alkylamines. *ACS Catal.* **2021**, *11* (11), 6416−6430.
(31) Qiu, L.; Polo-Garzon, F.; Daemen, L. L.; Kim, M.-J.; Guo, J.; Sumpter, B. G.; Koehler, M. R.; Steren, C. A.; Wang, T.; Kearney, L. T.; Saito, T.; Yang, Z.; Dai, S. Polyethylene Upcycling to Liquid Alkanes in Molten Salts under Neat and External Hydrogen Source-Free Conditions. *J. Am. Chem. Soc.* **2025**, *147*, 16207−16216.
(32) Becica, J.; Glaze, O. D.; Wozniak, D. I.; Dobereiner, G. E. Selective Isomerization of Terminal Alkenes to (Z)-2-Alkenes Catalyzed by an Air-Stable Molybdenum(0) Complex. *Organometallics* **2018**, *37* (3), 482−490.
(33) Dhaene, E.; Billet, J.; Bennett, E.; Van Driessche, I.; De Roo, J. The Trouble with ODE: Polymerization during Nanocrystal Synthesis. *Nano Lett.* **2019**, *19* (10), 7411−7417.
(34) Theofanis, P. L.; Goddard, W. A. I. Understanding β-Hydride Eliminations from Heteroatom Functional Groups. *Organometallics* **2011**, *30* (18), 4941−4948.
(35) Roesky, H. W. The Renaissance of Aluminum Chemistry. *Inorg. Chem.* **2004**, *43* (23), 7284−7293.
(36) Ranade, M. R.; Tessier, F.; Navrotsky, A.; Leppert, V. J.; Risbud, S. H.; DiSalvo, F. J.; Balkas, C. M. Enthalpy of Formation of Gallium Nitride. *J. Phys. Chem. B* **2000**, *104* (17), 4060−4063.
(37) Yeh, C.-Y.; Lu, Z. W.; Froyen, S.; Zunger, A. Zinc-Blende–Wurtzite Polytypism in Semiconductors. *Phys. Rev. B* **1992**, *46* (16), 10086−10097.
(38) Soni, U.; Arora, V.; Sapra, S. Wurtzite or Zinc Blende? Surface Decides the Crystal Structure of Nanocrystals. *CrystEngComm* **2013**, *15* (27), 5458−5463.
(39) Lide, D. R.; Baysinger, G.; Chemistry, S.; Berger, L. I.; Goldberg, R. N.; Kehiaian, H. V. *CRC Handbook of Chemistry and Physics*; CRC Press, 1995.
(40) Bao, Q.; Saito, M.; Hazu, K.; Furusawa, K.; Kagamitani, Y.; Kayano, R.; Tomida, D.; Qiao, K.; Ishiguro, T.; Yokoyama, C.; Chichibu, S. F. Ammonothermal Crystal Growth of GaN Using an NH4F Mineralizer. *Cryst. Growth Des.* **2013**, *13* (10), 4158−4161.
(41) Vícha, J.; Novotný, J.; Komorovsky, S.; Straka, M.; Kaupp, M.; Marek, R. Relativistic Heavy-Neighbor-Atom Effects on NMR Shifts: Concepts and Trends Across the Periodic Table. *Chem. Rev.* **2020**, *120* (15), 7065−7103.
(42) Okumura, H.; Ohta, K.; Ando, K.; Rühle, W. W.; Nagatomo, T.; Yoshida, S. Bandgap Energy of Cubic GaN. *Solid-State Electron.* **1997**, *41* (2), 201−204.
(43) Talapin, D. V.; Gaponik, N.; Borchert, H.; Rogach, A. L.; Haase, M.; Weller, H. Etching of Colloidal InP Nanocrystals with Fluorides: Photochemical Nature of the Process Resulting in High Photoluminescence Efficiency. *J. Phys. Chem. B* **2002**, *106* (49), 12659−12663.
(44) Kim, T.-G.; Zherebetskyy, D.; Bekenstein, Y.; Oh, M. H.; Wang, L.-W.; Jang, E.; Alivisatos, A. P. Trap Passivation in Indium-Based Quantum Dots through Surface Fluorination: Mechanism and Applications. *ACS Nano* **2018**, *12* (11), 11529−11540.
(45) Becker, P.; Wonglakhon, T.; Zahn, D.; Gudat, D.; Niewa, R. Approaching Dissolved Species in Ammonoacidic GaN Crystal Growth: A Combined Solution NMR and Computational Study. *Chem. - Eur. J.* **2020**, *26* (31), 7008−7017.
(46) Zhang, S.; Hintze, F.; Schnick, W.; Niewa, R. Intermediates in Ammonothermal GaN Crystal Growth under Ammonoacidic Conditions. *Eur. J. Inorg. Chem.* **2013**, *2013* (31), 5387−5399.
(47) Johnson, W. C.; Parsons, J. B. Nitrogen Compounds of Gallium. I, II. *J. Phys. Chem. A* **1932**, *36* (10), 2588−2594.
(48) Klemm, W.; Tilk, W.; Jacobi, H. Beiträge zur systematischen Verwandtschaftslehre. 58. Beiträge zur Kenntnis der Verbindungen des Galliums und Indiums. VIII. Die Ammoniakate der Galliumhalogenide. *Z. Anorg. Allg. Chem.* **1932**, *207* (2), 187−203.
(49) Roos, M.; Meyer, G. Zwei Galliumfluorid-Ammoniakate: Ga(NH3)F3 und Ga(NH3)2F3. *Z. Anorg. Allg. Chem.* **1999**, *625* (7), 1129−1134.
(50) Aleksandrov, S. E.; Kovalgin, A. Y.; Krasovitskii, D. M. UV-spectroscopic study of $GaCL_3$ NH_3 Pyrolysis. *Russ. J. Appl. Chem.* **1994**, *67* (5), 663−668.
(51) Aleksandrov, S. E.; Kovalgin, A. Y.; Krasovitskii, D. M. UV Spectroscopic Study of the Effect of Ammonia Additions on the Pyrolysis of Gallium Chloride Monoammoniate. *Russ. J. Appl. Chem.* **1995**, *68* (1), 6−9.
(52) Jacobs, H.; Schröder, F. O. Penta-Ammoniates of Aluminium Halides: The Crystal Structures of AlX3·5NH3 with X = Cl, Br, I. *Z. Anorg. Allg. Chem.* **2002**, *628* (5), 951−955.
(53) Srivastava, V.; Liu, W.; Janke, E. M.; Kamysbayev, V.; Filatov, A. S.; Sun, C.-J.; Lee, B.; Rajh, T.; Schaller, R. D.; Talapin, D. V. Understanding and Curing Structural Defects in Colloidal GaAs Nanocrystals. *Nano Lett.* **2017**, *17* (3), 2094−2101.
(54) Ondry, J. C.; Zhou, Z.; Lin, K.; Gupta, A.; Chang, J. H.; Wu, H.; Jeong, A.; Hammel, B. F.; Wang, D.; Fry, H. C.; Yazdi, S.; Dukovic, G.; Schaller, R. D.; Rabani, E.; Talapin, D. V. Reductive Pathways in Molten Inorganic Salts Enable Colloidal Synthesis of III-V Semiconductor Nanocrystals. *Science* **2024**, *386* (6720), 401−407.
(55) Reid, A. F.; Mills, R. Vacuum Drying of Iodine with Molecular Sieves. *J. Inorg. Nucl. Chem.* **1964**, *26* (5), 892−895.
(56) Washington, R. A.; Naldrett, S. N. Preparation of Pure, Dry Iodine. *J. Am. Chem. Soc.* **1955**, *77* (16), 4232.
(57) Brewer, F. M.; Goggin, P. L.; Reddy, G. S. Oxyhalides of Gallium. *J. Inorg. Nucl. Chem.* **1966**, *28* (2), 361−364.
(58) Jacobs, H.; Noecker, B. $AlCl_3$ $3NH_3$ - a Compound with the Crystal Structure of a Tetraammine Dichloro Aluminum-Diammine Tetrachloro Aluminate: $[AlCl_2(NH_3)_4]^+[AlCl_4(NH_3)_2)]^-$. *Z. Anorg. Allg. Chem.* 1993, *619*, 73−76.
(59) Jacobs, H.; Noecker, B. $AlCl_3{\cdot}2NH_3$ - A Compound with the Crystal Structure of a Tetraammine Dichloroaluminumtetrachloroaluminate - $[AlCl_2(NH_3)_4]^+AlCl_4]^-$. *Z. Anorg. Allg. Chem.* 1992, *614*, 25−29.